POLITECNICO DI TORINO
Repository ISTITUZIONALE

Enhanced CO2 Absorption in Organic Solutions of Biobased Ionic Liquids

Original
Enhanced CO2 Absorption in Organic Solutions of Biobased Ionic Liquids / Davarpanah, Elahe; Hernández, Simelys; Latini, Giulio; Pirri, Candido Fabrizio; Bocchini, Sergio. - In: ADVANCED SUSTAINABLE SYSTEMS. - ISSN 2366-7486. - ELETTRONICO. - (2020), p. 1900067. [10.1002/adsu.201900067]

Availability:
This version is available at: 11583/2773141 since: 2020-02-06T10:48:12Z

Publisher:
Wiley

Published
DOI:10.1002/adsu.201900067

Terms of use:

This article is made available under terms and conditions as specified in the corresponding bibliographic description in the repository

Publisher copyright

(Article begins on next page)

15 October 2024

Original Paper (citation information):

Adv. Sustainable Syst.2020, 4, 1900067

© 2019 WILEY-VCH Verlag GmbH & Co. KGaA, Weinheim

Enhanced CO_2 Absorption in Organic Solutions of Biobased Ionic Liquids

Elahe Davarpanah, Simelys Hernández, Giulio Latini, Candido Fabrizio Pirri, and Sergio Bocchini**

Solutions of biobased ionic liquids (ILs) for recovering CO_2 from industrial flue gas are investigated. Four CO_2 task-specific choline-based amino acids ([Cho][AA]): Alanine, Glycine, and, for the first time, Proline and Serine are tested. The drawbacks related to the high viscosity of these ILs are limited by applying dimethyl sulfoxide (DMSO) as a solvent, which is chosen because it is a polar aprotic liquid with a low toxicity, low vapor pressure, and relatively low price. The choline-based amino acids synthesized in this study have good absorption capacities (up to 0.3 mol CO_2/mol IL, with only 12.5 wt% IL in DMSO) that represent the best performance of CO_2 task-specific IL solutions to date. These solutions are competitive due to their low cost, low environmental impact, easy processability (due to their low viscosity) and good regenerability for the production and storage of pure CO_2.

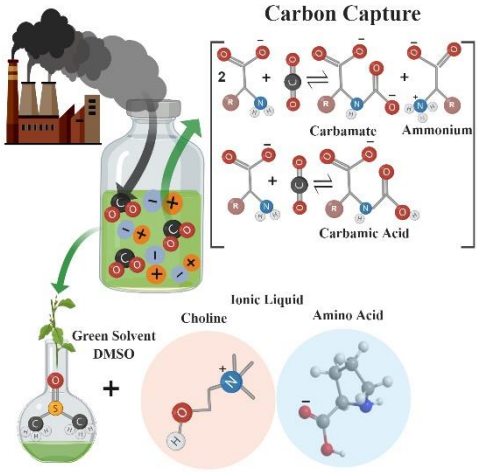

Enhanced CO_2 absorption in organic solutions of Bio-based ionic liquids

Elahe Davarpanah,[a] Simelys Hernandez[a,b], Giulio Latini,[b,c] Candido Fabrizio Pirri [b,c] and Sergio Bocchini*[b]*

E. Davarpanah, Dr. S. Hernandez
Catalytic Reaction Engineering for Sustainable Technologies (CREST) Group
Department of Applied Science and Technology (DISAT)
Politecnico di Torino

Dr. S. Hernandez, G. Latini, Prof. C.-F. Pirri, Dr. Sergio Bocchini
Center for Sustainable Future Technologies (CSFT@Polito)
Istituto Italiano di Tecnologia
Via Livorno 60, 10144, Turin

G. Latini, Prof. C.-F. Pirri
Department of Applied Science and Technology (DISAT)
Politecnico di Torino
Corso Duca degli Abruzzi 24, 10129, Turin

E-mail: simelys.hernandez@polito.it, sergio.bocchini@iit.it

Keywords: Amino acid-based ionic liquid • CO_2 capture • CO_2 Absorption mechanism • Organic DMSO solvent • Regenerability

Abstract

Solutions of bio-based ionic liquids (ILs) for recovering CO_2 from industrial flue gas are investigated. Four choline-based amino acids ([Cho][AA]): Alanine, Glycine, Proline, and Serine, that are task-specific for this purpose are tested. The drawbacks related to the high viscosity of these ILs were limited by applying DMSO as a solvent, which is chosen because it is a polar aprotic liquid with low toxicity, low vapor pressure, and relatively low price.

The choline-based amino acids synthesized in this study present aspiring absorption capacities (~ 0.3 mol CO_2/mol IL, with only 12.5 wt% IL in DMSO) and represent the best performing of task-specific ILs solutions at the state-of-art. These solutions are potentially competitive due to their low cost, low environmental impact, easy processability (due to their low viscosity) and good regenerability for the production and storage of highly pure CO_2.

1. Introduction

Climate change has been correlated with a strong increase in anthropogenic CO_2 emissions over the last century.[1] Thus, many research projects aim to limit these emissions by different processes. The first step often consists in the separation of CO_2 from the source stream, e.g. flue gases, to concentrate and purify it for further processing. Hence, CO_2 separation has a prominent role in the field of climate change mitigation.[2]

CO_2 separation is applied in carbon capture and storage concepts (CCS) in Integrated Gasification Combined Cycle units (pre-combustion carbon capture), fossil fuel power plants [3–5] and in the field of biomass conversion. Future applications for CO_2 separation technologies are presumed to be within the so-called carbon capture and utilization (CCU) route.[6–8] The idea is to exploit CO_2 as a raw material for further chemical or industrial use and, thus, to valorize it by its recycling. In the long term, CCU aims the development of a circular economy concept with neutral carbon emissions.

Absorption is one of the main techniques used for CO_2 capture [9], it relies on either chemical or physical interactions between the solvent and the solute CO_2. In physical absorption, intermolecular forces, such as Coulomb, Van-der-Waals or other dispersion forces dominate the solute-solvent interactions. In chemical absorption, CO_2 chemically reacts with the solvent molecules and forms covalent bonds. Due to their stoichiometric reaction with CO_2, the CO_2 absorption capacity is very high, already at low CO_2 partial pressures. Chemical absorption is particularly appropriate if CO_2 is

to be recovered from flue gas streams with relatively low concentrations. Major advantages of chemical absorption processes are the high selectivity for CO_2 and the high achievable gas product purity.

The most commonly used chemical absorbents are amines (15-60 wt%) in aqueous solutions (*i.e.* typical loading of 0.5 mol CO_2/mol amine for monoethanolamine, MEA). Amines have some drawbacks like a high corrosion rate at high concentrations, the outlet purified gas contains a high-water amount, the energy demand for their regeneration is high and they suffer from high evaporation losses.[10] Indeed, the reverse chemical reaction requires considerable activation energy that is commonly supplied by increasing the temperature of the absorbent. When a volatile absorbent is used, it must be either condensed from the purified gas stream or replenished with the consequent rise of operative costs. Therefore, improvement of the absorption medium e.g. decreasing the volatility without losing the high loading of the absorbent phase is the primary research interest in physical and chemical absorption technologies.

Since the 1990s, low-melting salts have gained increasing interest for application as alternative absorbents in a wide field of chemical processes. For salts with melting points below 100 °C, the term ionic liquid (IL) has been coined. As ILs are built up from an organic cation and an inorganic or organic anion, there is a vast variety of possible structures. Over the last years, a plethora of ILs and their mixtures have been investigated and many reviews have been published in the field. Their major positive features are their tunability, stability and low vapor pressure.[11] Their stability and tunability allows ILs to be designed according to the specific needs of an application (task-specific ILs, TSILs) and hence make them more flexible than conventional absorbents. A second strong point is that ILs mostly exhibit very low to negligible vapor pressures thanks to their ionic nature. This renders ILs

particularly attractive for applications where evaporation of the absorbent should be avoided, thus decreasing energy duties in the regeneration columns and in the downstream condenser.

Many studies aimed at improving the absorbent performance by systematically varying IL structures and analyzing the effect on CO_2 solubility and selectivity have been performed. Among those, ILs that have shown promising results are fluorinated, N-functionalized (amine-functionalized or amino acid-based), carboxylate-based, reversible and protic ILs. In general, functionalization of the anion is reported to have a greater influence on performance than of the cation. However, functionalization often brings about stronger intermolecular interactions resulting in a higher viscosity. This, in turn, leads to a fall of diffusion coefficient by one or two orders of magnitude and, hence, to an unfavorable mass transfer behavior.

To resolve the issues of high viscosity and absorbent evaporation losses, ILs have been used in solution with other liquids with a high boiling point (e.g. polyethylene glycol) [12] or supported on porous inert material.[13,14] This practice of mixing ILs with common industrial solvents reduce the cost of using ILs, which represent the ILs main drawback (*i.e.* their high price).Furthermore, ILs are generally referred to as “green solvents”, but the most common cations (e.g. imidazolium and pyridinium) and anions (that are often fluorine-based) do not show good biodegradability and biocompatibility.[13,14] Thus, ions derived from metabolic molecules are possible environmental-friendly alternatives, e.g. choline (a proved non-toxic and biocompatible cation) [15–17] and amino acids (AAs, renewable, biodegradable, biocompatible and naturally-abundant anions). Since every AA contains amine functionalities, AA based ILs (AAILs) are in principle optimal task-specific anions to produce ILs for CO_2 absorption.[18] As an example, our recent study proved that solution in

dimethyl sulfoxide (DMSO) of choline glycinate [Cho][Gly] and prolinate [Cho][Pro] have high absorption capacity and molar efficiency at low relative pressure 0.2 bar.[19]

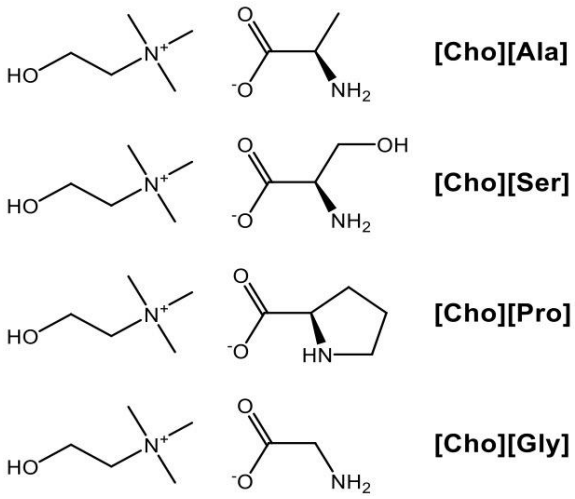

Scheme 1. Chemical structures of the four synthesized [Cho][AA] ILs.

In this study, the CO_2 absorption performance of four bio-based TSILs for industrial flue gas treatment was investigated. The four choline-based amino acids ([Cho][AA]) shown in **Scheme 1** were the TSILs tested for this purpose. An alternative to water, which has been employed as a solvent in most of the previous works, here we report the ILs application in solution with dimethyl sulfoxide (DMSO), a low vapor pressure organic solvent with a high boiling point (*i.e.* low volatility). DMSO was also chosen since it is a polar aprotic liquid, with low toxicity and a relatively low price. Due to those characteristics, DMSO is an advantageous solvent for ILs for maintaining low operative costs, energy duties and solvent losses during the regeneration process. The CO_2 absorption capacity of the [Cho][AA]s-DMSO solutions was calculated by monitoring the dynamic behavior of the system during the absorption process. The chemical interactions of such ILs and CO_2 were evaluated through IR analysis to identify which chemical species are formed and to explain the CO_2 desorption behavior of these systems. This study envisages how to address the regenerability of [Cho][AA]s ILs solutions, which is an important issue to face for industrial applications.

Results and Discussion

2.1. Synthesis of the [Cho][AA] ILs

The synthesis of [Cho][AA] ILs usually relies on the water solution of choline hydroxide, [Cho][OH].[20–22] In fact, [Cho][OH] solution, which can be purchased or obtained from choline chloride [Cho][Cl] and AgO_2, is a convenient starting reagent for AAILs synthesis *via* acid-base titration. Such synthesis method leads to the production of ILs with very high purity without any byproduct. However, the [Cho][OH] solution is corrosive, reactive and more expensive than plain [Cho][Cl] and its titration procedure is very long. To overcome these drawbacks and to achieve large-scale synthesis production for industrial application, in this paper, a different synthetic approach was employed.[19] [Cho][AA] ILs were obtained *via* ionic metathesis between potassium AA salts and [Cho][Cl] in ethanol. More experimental details and the chemical characterizations (NMR, ATR-IR, TG) demonstrating the proper synthesis of the ILs are reported in Sections S1 to S4 in the Supporting Information (SI). The good solubility of the ILs and the very scarce solubility of KCl [23] in the solvent was exploited to separate the IL from the byproduct, so obtaining a high purity. Moreover, the ionic metathesis methodology employs a cheap [Cho][Cl] reagent and can achieve high throughput, both aspects that are of main importance for industrial application.

2.2. Density and viscosity measurements

Different chemo-physical properties should be considered while testing new absorbents for CO_2 capture. Viscosity is one of the most important parameters from the practical viewpoint because it influences mass transport phenomena, *i.e.* CO_2 diffusion in the liquid, pressure drops for circulation of the liquid in the absorption plant and, consequently, energy consumption. [Cho][AA] ILs are notoriously very viscous [24], and consequently, CO_2 capture is not effective because of the poor gas

diffusion into these liquids. Therefore, their dilution in a proper solvent is a strategy that can be employed to overcome the viscosity related issues.

With that purpose, in this work, we first evaluated the performance of a [Cho][AA] IL diluted in DMSO at different concentrations (see Section S5 in the SI). From those tests, we verified that the addition of DMSO improved the CO_2 absorption rate of ILs. The best performance was obtained with a 12.5 wt% solution of [Cho][Gly]. Thus, this concentration was used to evaluate the dynamic of the CO_2 absorption process in different [Cho][AA]-DMSO solutions. **Table 1** reports the density and viscosity values of the pure ILs and DMSO (reference values) at 20°C in comparison to the 12.5 wt% IL-DMSO solutions.

Pure ILs exhibit density values in between 1.13 and 1.20 g/cm^3. As expected, the density (ρ) values are reduced after dilution in DMSO and settled at around 1.1 g/cm^3. However, the highest effect was observed for the viscosity (η) values that experienced a huge decrease upon dilution of the ILs in DMSO. Indeed, the IL-DMSO solutions display viscosity values in between 3.7 and 3.9 cP, not so far from pure that of DMSO (2 cP); whereas pure ILs show viscosities that are 3-4 orders of magnitude higher (10^3-10^4 cP).[18]

Table 1. Viscosity and density (at 20°C) of pure [Cho][AA] ILs and solutions of 12.5 wt.% [Cho][AA] ILs in DMSO.

	Pure substances		IL-DMSO 12.5%w/w	
	ρ (g/cm^3)	η (cP)	ρ (g/cm^3)	η (cP)
[Cho][Ala]	1.133 [a]	1051 [a]	1.106±0.036	3.76±0.12
[Cho][Ser]	1.204 [a]	21319 [a]	1.104±0.036	3.77±0.19

[Cho][Pro]	1.140 [a]	15298 [a]	1.110±0.036	3.89±0.13
[Cho][Gly]	1.158 [a]	2313 [a]	1.110±0.036	3.88±0.18
DMSO	1.098±0.035	2.01±0.15	-	-

[a] De Santis et al. [25]

2.3. Absorption of CO_2 with a solution of [Cho][AA]s in DMSO

The breakthrough curves for the CO_2 absorption in the [Cho][Ala], [Cho][Ser], [Cho][Pro] and [Cho][Gly] solution DMSO were measured at a constant temperature of 20 °C and a pressure of 1 bar, by bubbling 17 vol% CO_2 in Ar in a CSTR absorption reactor. The gas was flowed into the system until arriving at the saturation point. Afterward, desorption behavior was evaluated by heating the IL solutions until 65 °C under a constant Ar flow (see experimental section). Such absorption and desorption processes were repeated to investigate the regenerability and efficiency of ILs solutions. The results of these experiments are presented in **Figure 1** for two sequential cycles of absorption (black data) and desorption (red data), showing the concentration of CO_2 in the reactor outlet normalized by its inlet concentration.

In the first absorption cycle the CO_2 absorption uptake of the ILs decreased in the order [Cho][Ala] > [Cho][Pro] > [Cho][Ser] > [Cho][Gly]. During the 2nd and 3rd cycles, the absorption performance of the [Cho][Ala] (that was the best IL in the 1st cycle) was conspicuously reduced (~67%) and then arrived at a steady-state value of ~0.29 mol CO_2/mol IL. For the other [Cho][AA] solutions, there was an absorption decrease from the 1st to the 2nd cycle of approximately 48%, 43% and 33% for the [Cho][Pro], [Cho][Ser] and [Cho][Gly], respectively. However, the latter IL-DMSO solutions revealed competitive performances as their absorption efficiency reported a few reductions (<12% variation)

during the last two cycles and their absorption capacity was slightly superior to the [Cho][Ala] (0.30 to 0.33 molCO_2/mol IL).

The normalized CO_2 absorbed (Ads) and desorbed (Des) amounts from each [Cho][AA]s solution during the 1st and 2nd cycles are indicated in **Table 2** in terms of mol CO_2/mol IL. These values were calculated by integrating the area under the CO_2 absorption-desorption curves of each [Cho][AA] IL. The absorption values calculated in mol CO_2/kg ILs are and their relevant desorption efficiencies were also calculated and are reported in the Sections of S6 and S7 of the SI, respectively.

The physical state of all [Cho][AA] ILs was monitored before and after each absorption tests. The presence of a white precipitate was evidenced for some of the amino acids after the CO_2 absorption, in particular for the [Cho][Ala] (see Section S8 in the SI). The formation of a white precipitate in [Cho][Gly] and its absence in [Cho][Pro] was also observed, in agreement with previous observations from our group.[19] Hence, the significant CO_2 uptake variation during different absorption-desorption cycles can be explained by the formation of this white precipitate, after the 1st absorption cycle.

Table 2. Absorption capacities of [Cho][AA]s solutions through three cycles.

Absorption / Desorption Capacity (mol CO_2 / mol IL)					
	Cycle 1		Cycle 2		Cycle 3
	Ads	Des	Ads	Des	Ads
[Cho][Ala]	0.866	0.314	0.510	0.214	0.288
[Cho][Pro]	0.659	0.263	0.344	0.290	0.301
[Cho][Ser]	0.624	0.221	0.358	0.298	0.333

[Cho][Gly]	0.559	0.170	0.371	0.331	0.326

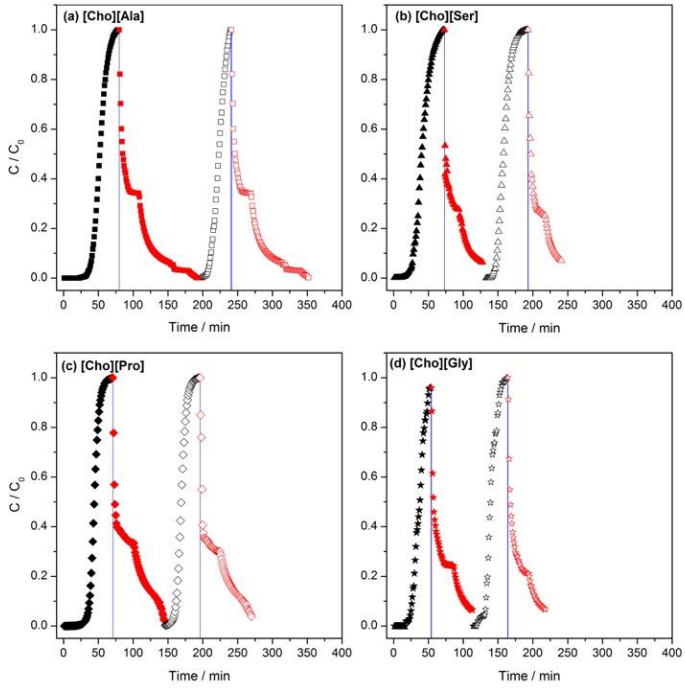

Figure 1. The breakthrough absorption curves (black) and desorption (red) profiles of CO_2 in the [Cho][AA]s ILs solutions in DMSO. The graph represents the corresponding data related to a) [Cho][Ala], b) [Cho][Ser], c) [Cho][Pro] and d) [Cho][Gly] during two complete cycles. The y-axis is showing the CO_2 concentration in the outlet normalized by its initial concentration.

To investigate the absorption process from a chemical point of view and to elucidate the origin of that precipitate, additional characterizations were performed. The IR spectra of each IL-DMSO solution were acquired before and after the CO_2 absorption experiments and are reported in **Figure 2**. The spectra modifications after CO_2 exposition are a clear signal that all four IL-DMSO solutions undergo chemical modifications. In the specific, the peak related to the carboxylate group (~1600 cm^{-1}) slightly shifts to higher wavenumbers (see **Figure 2** (a), (c), (d), blue dotted line 1) or modify

its shape (see **Figure 2** (b), blue dotted lines 1 and 2), which can be attributed to the formation of the carbamate moiety. In addition, a new signal appears at ~1690 cm^{-1} (see line 2 in **Figure 2** (a), (c), (d) and line e in part (b)), related to the formation of the carbamic acid species. The spectra evolution is in accordance with our previous study. [19] Thus, the CO_2 fixation occurs via the formation of two different species, carbamate, and carbamic acid. Indeed, two different reactions occur, as depicted in **Scheme 2** Carbamate moiety form together with ammonium counter-ion, by the reaction of two amines with one CO_2 molecule (see **Scheme 2**. part (a)), whereas carbamic acid forms *via* 1:1 reaction stoichiometry (see **Scheme 2.** part (b)).

Concerning the formation of the precipitates, they were analyzed by IR spectroscopy which revealed to be the AA of the [Cho][AA] ILs. During the CO_2 absorption, the ILs lose their composition since part of the AA anions precipitate. To explain the reason for the AA precipitation it is worth to focus on the 2:1 stoichiometry absorption (**Scheme 2.** part (a)). Upon ammonium formation, the AA becomes electrically neutral, since it acquires a positive charge, *i.e.* it is now in a zwitterionic form. On the other side, the carbamate formation produces an AA with a double negative charge. This double negative charge can be counterbalanced either by the ammonium-bearing AA or by an addition choline cation. Because of the scarce solubility of AAs in DMSO, the zwitterionic AAs can precipitate and the whole electroneutrality is still maintained. This AAs precipitates formation can be considered as the reason for the loss of absorption capacity, the effect of which can be removed by prolonging the regeneration step at a higher temperature. For instance, the regeneration of the ILs from these AAs could be possible through several days of heating under vacuum (being the process is thermodynamically favored) but the high energy consumption would make the process uneconomic.

The desorption process occurred using Ar as an inert gas with a flow rate of 100 mL/min. During the process, the system was heated up to 65 °C with a ramp of 1.3 °C/min. In the 1st cycle, the CO_2 desorption efficiencies were different for all the [Cho][AA] ILs (between 30 and 40%, see **Table S3** in the SI) but have a relation to their absorption rate. Instead, in the 2nd cycle the [Cho][Pro], [Cho][Ser] and [Cho][Gly] solutions released a higher CO_2 quantity (desorption efficiency ~ 85%) than the [Cho][Ala] (desorption efficiency ~ 42%) at the same operating conditions.

Among all tested solutions, [Cho][Gly] revealed the highest desorption efficiency in the 2nd cycle with the desorption performance equal to 89% which is in agreement with the study by Shengjuan Yuan et al.[24] However, the operating temperature used in their work (110 °C) is much higher than in our study (65 °C).[24]

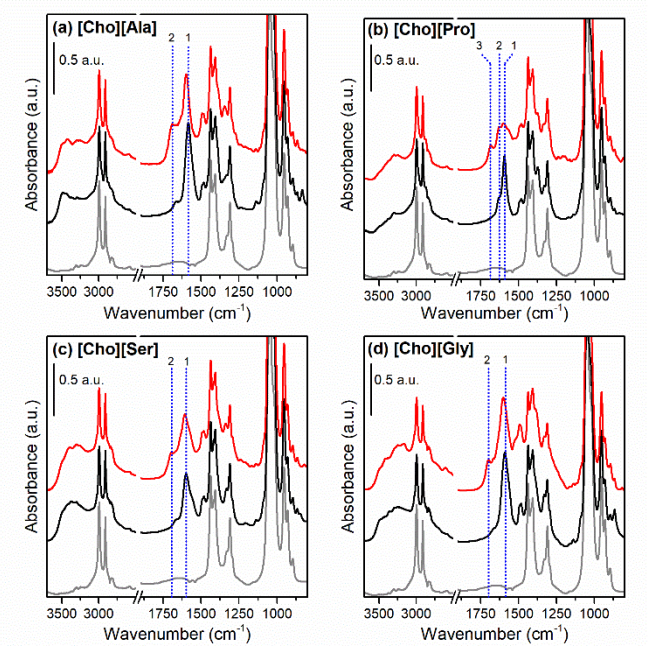

Figure 2. ATR-IR spectra of pure DMSO (grey curve) and IL-DMSO solutions before (black curve) and after CO2 absorption (red curve). Part (a), (b), (c) and (d) report the data related to the DMSO

solution with [Cho][Ala], [Cho][Pro], [Cho][Ser] and [Cho][Gly], respectively. The blue dotted lines in each part highlight the relevant modification of the spectra after CO_2 absorption.

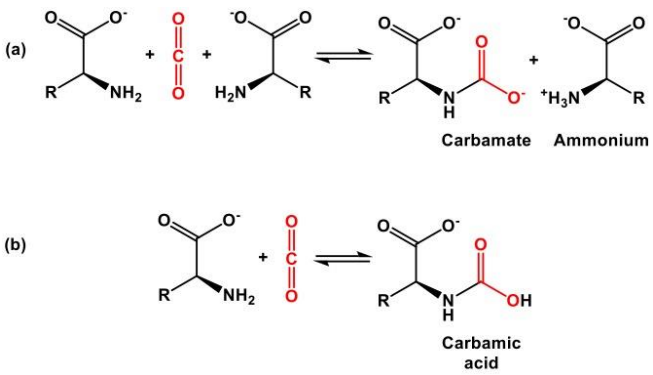

Scheme 2. Possible reaction paths of CO_2 and amines. Part (a): formation of ammonium-carbamate species via two amines per one CO_2 (2:1) stoichiometry reaction; part (b): formation of carbamic acid species via one amine per one CO_2 (1:1) stoichiometry reaction.

The 1st cycle desorption curves of each [Cho][AA] IL are reported in **Figure 3**. The shape of the curves are similar and three regimes can be distinguished: (i) in the first minutes, the headspace emptying is responsible for the steep decrease in the CO_2 concentration; (ii) after, the CO_2 is released from the carbamic acid moiety (see **Scheme 2** (a)), which is reversible at room temperature, the CO_2 desorption rates decrease and the CO_2 concentration values reach a plateau at ~25-30 min; (iii) then, the CO_2 desorption speeds again, since the temperature is enough high to permit CO_2 release from the carbamate species (see **Scheme 2** (b)), which are more stable than carbamic acid.[19] The temperatures at which the CO_2 release from carbamate become relevant where found to be 38°C, 34°C, 40°C and 43°C for [Cho][Ala], [Cho][Ser], [Cho][Pro], and [Cho][Gly], respectively.

Hence, it is worth to underline that the amounts of captured and released CO_2 are not the same because of the desorption temperature used, which was chosen to preserve the [Cho][AA] IL from

progressive aging. The total release can be achieved by increasing the temperature or by extending desorption time. In addition, the observed decrease in the absorption capacity from 1st to 2nd cycle is due to the formation of the precipitate for certain amino acids, which in the absence of CO_2 can be dissolved through de-saturation of the solution from zwitterionic amino-acid through reversible reaction as shown in **Scheme 2**. However, dissolution is slow because of the low total solubility. Thus, this CO_2 can be considered as irreversibly absorbed since the phenomena lead to a decreased amount of available CO_2-reactive amines.

To the best of our knowledge, the here reported solutions of TSILs in DMSO show better performances than other ILs solutions reported in the literature.[26–29] The CO_2 absorption capacity for [Cho][AA]s reported in **Table 2** were compared to the results obtained by Biao Li et al. [30] and Shengjuan Yuan. et. al [24] for the same groups of [AA]s in a 5 to 30 wt% solution in water. Such results showed a higher absorption capacity during the 1st cycle for [Cho][AA] in DMSO (~2 times superior) with respect to the same ILs solution in water (~10 wt%) at the temperature of (30 and 35 °C). However, the reversible adsorption/desorption capacities of different solutions reported for the 3rd cycle presented similar CO_2 absorption performances. Indeed, the final absorption capacity in terms of mol CO_2/mol [AA]s for similar concentration is strictly below 0.5 for the 2 to 3 times higher CO_2 partial pressure.

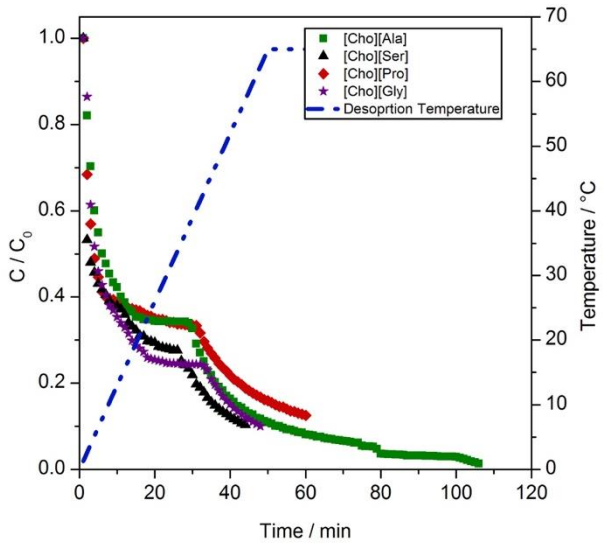

Figure 3. Desorption curves after the 1st absorption cycle of the [Cho][AA]-DMSO solution (stripping the gas of Ar with a flow rate of 100 ml/min and a heating rate of 1.3 °C/min up to 65°C).

It is necessary to mention that the studies performed previously did not repeat the absorption tests for all of the [Cho][AA]s and reported the results only for the best ILs with highest CO_2 uptake. For instance, Shengjuan Yuan. et. al [24] investigated the desorption efficiency of only aqueous [Cho][Gly] at a higher temperature (110 °C). For other types of ILs instead, the absorption results were only reported for the 1st cycle, without evaluating the absorption capacity loss after CO_2 desorption. Moreover, a higher CO_2 absorption rate was observed for [Cho][AA]s in DMSO solution respecting to the results of preceding works with the possibility of water present in the CO_2 desorption process. The same amino acids were also tested with Polyethylene glycol with a molecular weight of 200 and the viscosity of about 30 times higher than DMSO.[31] In the same condition as underlined by the kinetic reported for CO_2 absorption where the time for CO_2 capture are 2-3 times higher even considering the higher temperature used (at list 35°C).[12]

3. Conclusion

This study introduced the application of choline-based ILs in solution with an organic solvent (DMSO) as a promising approach for CO_2 separation from flue gases. The viscosity of the ILs significantly diminished through their dissolution in DMSO, thus the limits to CO_2 diffusion into the system are decreased. The four [Cho][AA] ILs synthesized in this work: [Cho][Ala], [Cho][Ser], [Cho][Pro], and [Cho][Gly] were tested to measure their CO_2 absorption capacity, from a synthetic flue gas (17 vol% CO_2 in Ar), through different absorption/desorption cycles.

The absorption results indicated a decrease in the CO_2 loading capacity of ILs from the 2nd absorption/desorption cycle. IR spectroscopy analysis showed that such a decrease in the CO_2 absorption performance is due to the formation of carbamic acid species, which appeared in the solution as precipitates. Among the studied ILs, [Cho][Gly], [Cho][Pro] and [Cho][Ser] revealed comparable absorption efficiencies of about 0.3 mol CO_2/mol ILs.

The choline-based amino acids synthesized in this study reported aspiring absorption capacities. Even though their behavior for CO_2 absorption became stable after the secondary runs, on the contrary to what has been reported in previous works were only the first absorption cycle has been studied. The drawbacks related to the high viscosity and high cost of ILs were here limited by applying DMSO as a solvent.

With respect to previous reports, the here reported bio-based TSILs solutions or combine a series of additional advantages: low cost, low environmental impact, easy processability because of their low viscosity, low energy consumption and high regenerability (up to 89% desorption efficiency at steady-state conditions). These characteristics make of these [Cho][AA]-DMSO solutions the most competitive IL-based absorbents at the state-of-the-art for industrial flue gas treatment, which would allow the CO_2 capture of for its subsequent use as raw material with high purity.

4. Experimental Section

4.1. Preparation of [Cho][AA]s solutions

The ILs were prepared using a previously developed methodology [16]. In a 250 mL flask, 0.5 mol of the chosen AA and an excess of potassium hydroxide (30.9 g, Carlo Erba, purity ≥85%) are mixed at RT in ethanol (200mL, supplied by Merck, purity ≥99.8%) under stirring. The potassium salt of the AA is formed, the suspension turned white while the excess of potassium salt precipitates. Once the potassium hydroxide pellets dissolved completely (c.ca 2 h), the choline chloride (69.8 g, supplied by Alfa Aesar, purity ≥98%) was added. The mixture was left under stirring for 4 h. The potassium salt dissolves and potassium chloride precipitated as white powder leaving choline AA ILs in solution upon the exchange of K^+ by choline cations. The potassium chloride crystals were separated by centrifugation, and then ethanol and water produced during the reaction were removed using a rotary evaporator. The so obtained ILs (hereafter referred to as [Cho][AA]) are outgassed under dynamic vacuum at 30°C overnight to totally remove the possible residual ethanol and water. Four different amino acids were employed: L-Alanine, L-Proline, L-Serine, and Glycine. The success of the syntheses was confirmed by 1H-NMR and ATR-IR spectroscopy. For the sake of brevity, 1H-NMR data are reported in the supplementary information. The chemical structure of the four [Cho][AA] ILs is reported in **Scheme 1**.

Additionally, the ILs were degassed for 10 h by a vacuum pump under constant agitation to remove the dissolved gases and impurities. The [Cho][AA]s solutions were prepared by mixing ILs with DMSO using an electronic analytical balance at a weight ratio of 12.5 wt.%.

4.2. Characterization

ATR FT-IR spectroscopic measurement: pure ILs and IL-DMSO solution, before and after CO_2 absorption, were characterized using a Bruker Tensor II spectrophotometer equipped with DTGS detector and single-reflection Bruker Platinum ATR accessory with the diamond crystal. All the spectra were recorded at a resolution of 2 cm^{-1}, 32 scans in the spectral range 3800-600 cm^{-1}.

Density: densities of the IL-DMSO solutions were calculated using a Gay-Lussac pattern density bottle (volume ~5 mL). The volume of the empty density bottle was previously calculated using water. Then, the weight of the density bottle filled with [Cho][AA]-DMSO solution was measured using an analytical balance. All the measures were conducted at 20°C.

A Cannon-Fenske viscometer was employed to measure the viscosities of the different [Cho][AA]-DMSO solutions. Once the tube was filled with the proper amount of sample, it was placed in a constant temperature bath (bath temperature 20°C). After 10 minutes, so the sample and the tube reached the equilibrium temperature, the efflux time was measured by means of the chronometer in order to calculate the kinematic viscosities. Dynamic viscosities were calculated using the density values previously measured with the density bottle.

4.3. CO_2 absorption and desorption measurements tests

The absorption experiments are designed to evaluate the CO_2 loading capacity of ionic liquids [Cho][AA]s in DMSO solution. The tests were carried out by bubbling a gas mixture with the composition of 17 vol% CO_2 and 83 vol.% Ar (considering flue gas composition) into the liquid phase consisted of 12.5 wt.% [Cho][AA]s in DMSO. The amount of solution used was 40 mL, filled half volume of the reactor. Therefore, the system response time due to the reactor headspace was calculated by monitoring the absorption profile of CO_2 in pure DMSO at the GC. The lab-scale set-up used is presented and described in detail in the supporting information (see Section S9 in the SI).

The complete process comprised of three consecutive operations absorption, desorption, and cooling. Before starting the tests, the system was inspected entirely for any gas leakage. During the test, the ILs solution was continuously stirred with a speed of 600 rpm to create uniformly disperse bubbles without forming any vortex. The total flow of the gas mixture used was 50 mL/min (CO_2 flow rate of ≈ 8 mL/min and the Ar flow rate of ≈ 42 mL/min). The CO_2 volume fraction in the outlet gas was analyzed by the GC until the CO_2 concentration of the gas at inlet and outlet of reactor became equal or the solution converted to saturate. The operating conditions for both processes are reported in **Table 3**.

Furthermore, the regeneration process was investigated after the IL-DMSO solution was saturated, by heating and purging the system at 65 °C with a flux of pure Ar (100 mL/min). The rate of temperature change for heating was held at 1.3 °C/min until the system temperature reached the set point. The solution was maintained stirred with a speed of 600 rpm along the process. The absorption process was completed once the concentration of the CO_2 in the out-flowing gas measured by GC reached 1 vol% of the CO_2 concentration at the inlet. Finally, the solution was cooled down to absorption operating temperature of 20 °C.

In addition, for realizing the viability of the IL-DMSO solution regeneration, which plays an important role in practical applications, the absorption and desorption process has been repeated for two additional cycles.

Table 3. Operating condition for absorption and absorption process.

Process	T (°C)	P (bar)	Flow Composition	Total Flowrate (mL/min)	CO_2 Concentration (vol%)
Absorption	20	1	CO_2 + Ar	50	17
Desorption	65	1	Ar	100	0

4.4. Absorption capacity theory

The absorbed amount of CO_2 in the solution of [Cho][AA]s and DMSO was calculated using the following equations [24]:

$$n_{CO2_{adsorbed}} = \int_{t0}^{tf} n_{CO2_{out}}(t).dt \quad (1)$$

$$n_{CO2_{out}(t)} = C_{CO2_{out}}(t).Q_{CO2_{out}}(t).(t-\Delta t) \quad (2)$$

Where: C_{CO2_out} (mol m^{-3}) is the concentration of the CO_2 recorded by GC at each time interval, Q_{CO2_out} (m^3 s^{-1}) is the volumetric flow rate of CO_2 at the reactor and Δt (s) is the time delay for GC. To understand the CO_2 absorption capacity of pure [Cho][AA]s, the amount of absorbed CO_2 by DMSO was subtracted from **Eq. 1**.

$$n_{CO2_{absorbed}} = \int_{t0}^{tf} n_{CO2_{out}}(t).dt_{[Cho][AA]+DMSO} - \int_{t0}^{tf} n_{CO2_{out}}(t).dt_{DMSO} \quad (3)$$

For instance, the pure loading capacity of [Cho][Pro] is calculated, as shown in

Figure 4, by integrating the absorption curve (orange curve) resulting from the difference between the CO_2 absorption test in DMSO (blue curve) and the CO_2 absorption test in the [Cho][Pro] (black curve). The integrated (gray) area will result in the amount of CO_2 absorbed by the [Cho][Pro].

Moreover, the molar CO_2 absorption capacities per moles of solution or moles of IL were, respectively, calculated by:

$$\alpha_{solution} = \frac{n_{CO2_{adsorbed}}}{n_{[Cho][AA]} + n_{DMSO}} \quad (4)$$

$$\alpha_{IL} = \frac{n_{CO2_{adsorbed}[Cho][AA]}}{n_{[Cho][AA]}} \quad (5)$$

4.5. Regeneration efficiency (η)

The regeneration efficiency expresses in **Eq. 6** shows the reversibility of the absorption process.

$$\eta = \frac{n_i}{n_0} \quad (6)$$

Where the n_0 is the moles of CO_2 absorbed in the fresh solution and n_i is the amount of CO_2 recovered in the absorption phase.

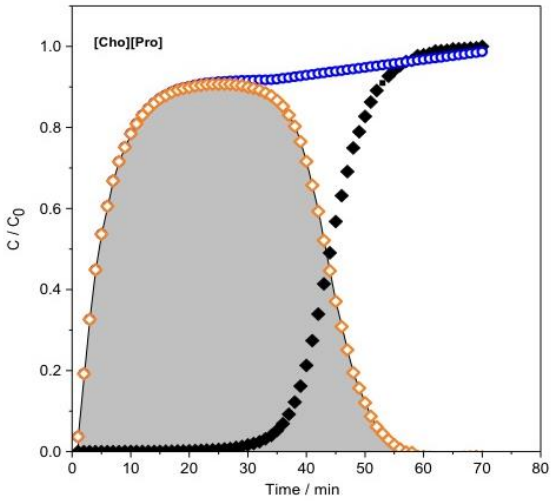

Figure 4. Absorbed CO_2 in pure [Cho][Pro] calculated by subtracting the DMSO absorption curve (Blue curve) from [Cho][Pro] in the solution curve.

References

[1] S. Topham, A. Bazzanella, S. Schiebahn, S. Luhr, L. Zhao, A. Otto, D. Stolten, *Carbon Dioxide*, Wiley-VCH Verlag GmbH & Co. KGaA, Weinheim, Germany, **2014**.

[2] M. T. M. Fischedick, K. Görner, *CO2: Abtrennung, Speicherung, Nutzung*, Ganzheitliche Bewertung Im Bereich Von Energiewirtschaft Und Industrie, Berlin, Heidelberg, **2015**.

[3] S. Schiebahn, *Effizienzoptimierte CO2 -Abtrennung in IGCC-Kraftwerken Mittels Wassergas-Shift-Membranreaktoren*, Schriften Des Forschungszentrums Jülich Reihe Energie & Umwelt / Energy & Environment, **2015**.

[4] I. International Energy Agency, *20 Years of Carbon Capture and Storage - Accelerating Future Deployment*, **2016**.

[5] M. Bui, C. S. Adjiman, A. Bardow, E. J. Anthony, A. Boston, S. Brown, P. S. Fennell, S. Fuss, A. Galindo, L. A. Hackett, J. P. Hallett, H. J. Herzog, G. Jackson, J. Kemper, S. Krevor, G. C. Maitland, M. Matuszewski, I. S. Metcalfe, C. Petit, G. Puxty, J. Reimer, D. M. Reiner, E. S. Rubin, S. A. Scott, N. Shah, B. Smit, J. P. M. Trusler, P. Webley, J. Wilcox, N. Mac Dowell, *Energy Environ. Sci.* **2018**, *11*, 1062.

[6] N. H. G. Anandarajah, N. Strachan, P. Ekins, R. Kannan, *Pathways to a Low-Carbon Economy:Energy System Modelling*, **2009**.

[7] P. Markewitz, W. Kuckshinrichs, W. Leitner, J. Linssen, P. Zapp, R. Bongartz, A. Schreiber, T. E. Müller, *Energy Environ. Sci.* **2012**, *5*, 7281.

[8] A. Goeppert, M. Czaun, G. K. Surya Prakash, G. A. Olah, *Energy Environ. Sci.* **2012**, *5*, 7833.

[9] S. Bocchini, C. Castro, M. Cocuzza, S. Ferrero, G. Latini, A. Martis, F. Pirri, L. Scaltrito, V. Rocca, F. Verga, D. Viberti, *J. Nanomater.* **2017**, *2017*, 1.

[10] C. De Conno, *GPSA Engineering Data Book [Gas Processing]*, Gas Processors Suppliers Association, Tulsa, Oklahoma, **2004**.

[11] N. V. Plechkova, K. R. Seddon, *Chem. Soc. Rev.* **2007**, *37*, 123.

[12] X. Li, M. Hou, Z. Zhang, B. Han, G. Yang, X. Wang, L. Zou, *Green Chem.* **2008**, *10*, 879.

[13] W. Gouveia, T. F. Jorge, S. Martins, M. Meireles, M. Carolino, C. Cruz, T. V. Almeida, M. E. M. Araújo, *Chemosphere* **2014**, *104*, 51.

[14] K. D. Weaver, H. J. Kim, J. Sun, D. R. MacFarlane, G. D. Elliott, *Green Chem.* **2010**, *12*, 507.

[15] B. E. Gurkan, J. C. de la Fuente, E. M. Mindrup, L. E. Ficke, B. F. Goodrich, E. A. Price, W. F. Schneider, J. F. Brennecke, *J. Am. Chem. Soc.* **2010**, *132*, 2116.

[16] Y. S. Sistla, A. Khanna, *Chem. Eng. J.* **2015**, *273*, 268.

[17] M. Petkovic, J. L. Ferguson, H. Q. N. Gunaratne, R. Ferreira, M. C. Leitão, K. R. Seddon, L. P. N. Rebelo, C. S. Pereira, *Green Chem.* **2010**, *12*, 643.

[18] Q.-P. Liu, X.-D. Hou, N. Li, M.-H. Zong, *Green Chem.* **2012**, *14*, 304.

[19] G. Latini, M. Signorile, V. Crocellà, S. Bocchini, C. F. Pirri, S. Bordiga, *Catal. Today* **2019**, DOI 10.1016/j.cattod.2018.12.050.

[20] S. De Santis, G. Masci, F. Casciotta, R. Caminiti, E. Scarpellini, M. Campetella, L. Gontrani, *Phys. Chem. Chem. Phys.* **2015**, *17*, 20687.

[21] Q.-P. Liu, X.-D. Hou, N. Li, M.-H. Zong, *Green Chem.* **2012**, *14*, 304.

[22] D.-J. Tao, Z. Cheng, F.-F. Chen, Z.-M. Li, N. Hu, X.-S. Chen, **2013**, DOI 10.1021/je301103d.

[23] S. P. Pinho, E. A. Macedo, *J. Chem. Eng. Data* **2005**, *50*, 29.

[24] S. Yuan, Y. Chen, X. Ji, Z. Yang, X. Lu, *Fluid Phase Equilib.* **2017**, *445*, 14.

[25] S. De Santis, G. Masci, F. Casciotta, R. Caminiti, E. Scarpellini, M. Campetella, L. Gontrani,

Phys. Chem. Chem. Phys. **2015**, *17*, 20687.

[26] B. Gurkan, B. F. Goodrich, E. M. Mindrup, L. E. Ficke, M. Massel, S. Seo, T. P. Senftle, H. Wu, M. F. Glaser, J. K. Shah, E. J. Maginn, J. F. Brennecke, W. F. Schneider, *J. Phys. Chem. Lett.* **2010**, *1*, 3494.

[27] J. Zhang, S. Zhang, K. Dong, Y. Zhang, Y. Shen, X. Lv, *Chem. - A Eur. J.* **2006**, *12*, 4021.

[28] C. Wang, H. Luo, H. Li, X. Zhu, B. Yu, S. Dai, *Chem. - A Eur. J.* **2012**, *18*, 2153.

[29] M. Aghaie, N. Rezaei, S. Zendehboudi, *Renew. Sustain. Energy Rev.* **2018**, *96*, 502.

[30] B. Li, Y. Chen, Z. Yang, X. Ji, X. Lu, *Sep. Purif. Technol.* **2019**, 128.

[31] J. Wu, C. Zhao, W. Lin, R. Hu, Q. Wang, H. Chen, L. Li, S. Chen, J. Zheng, *J. Mater. Chem. B* **2014**, *2*, 2983.